Simulation of Occupant Posture Changes due to Evasive Manoeuvres and Injury Predictions in Vehicle Frontal and Side Collisions.

Takao Matsuda, Katsunori Yamada, Shigeki Hayashi, Yuichi Kitagawa

Abstract This study investigated the influence of occupant posture changes due to evasive manoeuvres such as braking and steering on impact kinematics and injury values during collision using the human body finite element model. The muscle reaction due to spinal reflex was considered in the human body finite element model to realistically simulate the occupant posture change induced by deceleration or lateral acceleration of the vehicle. The occupant head moved forward due to braking while it moved laterally when steering. The influence of occupant posture change on injury values in frontal collision was relatively small. The injury values were affected by the occupant posture change in side collisions. The Head Injury Criterion value was high when the occupant head deviated from the centre of the airbag and came close to the interior parts. The Brain Injury Criterion value was high when the head was rotated from right to left. The effect of pre-crash seatbelt was also investigated. When the pre-crash seatbelt was activated, both forward and lateral motions of the occupant were reduced. The injury values were lowered in both frontal and side collisions by activating the pre-crash seatbelt.

Keywords evasive manoeuvre, human body FE model, occupant posture, pre-crash seatbelt, vehicle collision.

I. INTRODUCTION

In the vehicle crash safety regulation and assessment tests, occupant protection is evaluated by an anthropomorphic test dummy (ATD) in a designated seated position. According to the field accident data [1], about 60% of drivers made evasive manoeuvres such as braking and steering before the collision. The occupant posture may change from the initial position due to deceleration and/or lateral acceleration caused by the evasive manoeuvres. Studies were conducted to investigate driver's behaviours in evasive situations, resultant vehicle behaviours and occupant motions. Human volunteer subjects were used to characterise the driver's behaviour during braking and steering [2-3]. The vehicle behaviour was described as deceleration caused by braking and lateral acceleration generated by steering [4-5]. Human volunteer tests were conducted to analyse the forward motion of the occupant during braking [6]. Lateral motion of the occupant during lane change manoeuvres [7] and forward and lateral motion by braking and steering were also measured [8]. Few studies were conducted to investigate the influence of posture change on occupant impact kinematics and injuries in vehicle collisions. A rigid link model was used to simulate occupant posture change with braking and to estimate the influence on injury values in frontal collisions [9]. A finite element (FE) model of the human body was used to predict occupant injuries during frontal collisions as well as occupant posture change by Autonomous Emergency Braking (AEB) activation [10]. A common finding from those studies was that the occupant head and chest moved forward during braking but resulted in lower Head Injury Criterion (HIC) values compared to the case without braking. It was explained that early contact between the head and the airbag helped lower the HIC value. On the other hand, the change of chest G showed different trends in those studies. Few studies were conducted on the influence of the steering before the collision and the influence on the injuries in side collisions.

In recent years, active safety devices have been introduced to vehicles aiming at preventing collisions or mitigating their consequences by sensing forward obstacles. The pre-crash seatbelt (PSB) retracts the seatbelt by an electric motor built in the retractor when detecting forward obstacles. The PSB alerts a possibility of

T. Matsuda is Assistant Manager of Impact Biomechanics Group, Advanced CAE Division (Ph. +81 565 94 2292, fax. +81 565 94 2062, e-mail: takao_matsuda@mail.toyota.co.jp). K. Yamada is Assistant Manager, S. Hayashi is Group Manager and Y. Kitagawa, Ph.D., is Chief Professional Engineer at TOYOTA MOTOR CORPORATION in Toyota, Japan.

collision and removes an initial slack of the seatbelt. Another effect of PSB is to reduce the occupant posture change during evasive manoeuvres. The effect of PSB to reduce the posture change during braking was investigated using human volunteer subjects in the previous study [11]. However, the injury values at high speed collision cannot be studied in volunteer tests. The Hybrid-III dummy was used to measure the injury values in frontal collisions after activating AEB and PSB [5]. However, the capability of the Hybrid-lll dummy for simulating the occupant posture change has not been examined because it was developed for high-speed frontal crash tests. The objective of this study is to quantify the occupant posture change due to evasive manoeuvres (braking, left steering and right steering) and to estimate how it influences occupant impact kinematics and injury values in vehicle frontal and side collisions. The study uses the Total HUman Model for Safety (THUMS) for both pre-collision and collision simulations. The THUMS Version 5 was used for the pre-collision phase, and the THUMS Version 4 was used for the collision phase. The study also discusses possible effectiveness of PSB on injury mitigation.

II. METHODS

The simulations were performed using FE models. The LS-DYNA^{TM} V971 was used for the FE analysis solver. The THUMS was used to represent the occupant in the front left (driver) seat. A midsize male person with a height of 178.6 cm and a weight of 77.6 kg was assumed as the occupant. The simulation was divided into two phases. The first one was the pre-collision phase to simulate evasive manoeuvres such as braking and steering. The THUMS Version 5 AM50 Occupant Model (Fig. 1) was used to simulate occupant posture change due to evasion manoeuvres. The THUMS Version 5 can simulate the effect of muscle activation on the body posture and kinematics. The second one was the collision phase. Impact kinematics of the occupant and injury values were predicted using the THUMS Version 4 AM50 Occupant Model (Fig. 2). The THUMS Version 4 is capable of predicting injury values in vehicle collisions. The changed posture obtained in the pre-collision phase was used as the initial posture of the occupant in the collision phase. The compressive and tensile forces generated in the seat and the seatbelt calculated in the pre-collision phase were reproduced in the collision phase. The same scheme was used for the cases where the PSB was activated.

Occupant Model

The THUMS Version 5 has active muscle elements. A total of two hundred and sixty-two (262) major skeletal muscles were represented by one-dimensional truss elements with Hill-type muscle model. Muscle reaction can be simulated by activating the muscle elements using prescribed parameters and functions. The present study assumed that the occupant tried to maintain the initial posture automatically (spinal reflex) when the vehicle was suddenly decelerated or steered. The muscle activity was controlled group by group. Figure 1 shows ten (10) muscle groups contributing to the posture maintenance. The muscle force was generated according to the muscle activity ratio in the Hill type model. A function surface was defined based on the volunteer test data to describe the relationship between the muscle activity and the occupant posture change. The muscle activity ratio was given by the function surface when displacement and velocity change of the monitoring point were known. The head and T1 were monitored to characterise the occupant posture change. The validity of the method was previously conformed for simulating the occupant posture change due to braking [10]. In the present study, the validity of the method for the occupant posture change due to steering was examined. A dataset was selected for the validation in which a total of twenty-one (21) midsize male volunteers were measured for their posture changes during vehicle lane change manoeuvres [7]. The lane change started at a speed of 50 km/h and generated a peak acceleration of approximately 1 g (9.8 m/s^2) in the lateral direction. A common seat frame was used for the test, but the cushion part was replaced with a plate covered with artificial leather. The occupant posture change was measured by a three-dimensional motion capture system. The average physique of the volunteers (height: 179.2±4.6 cm, weight: 78.5±6.3 kg) was close to the AM50 body size and was representable with THUMS without scaling its dimensions. THUMS was seated on the seat model imitating the seat used in the test. An average time history curve of the vehicle lateral accelerations measured in the tests was given to the simulation model. Figure 3 compares the time history curves of the head and T1 lateral displacements between THUMS and the average response of the volunteer subjects. Both head and T1 displacement curves reached negative peaks at 0.6 second and positive peaks at 1.4 second. The negative peak value of the head was larger than that of T1 while the positive peak values were similar. This trend was found in both THUMS and volunteer test data. The software named Correlation and Analysis (CORA, Partnership for

Dummy Technology and Biomechanics, Germany) [12] was used to evaluate the fitting of two displacement time history curves. The rating result for the head displacement curves was 0.98 while that for T1 was 0.99, which were the highest grade specified in the relevant ISO standard [13]. When the head reached the maximum displacement point, its inclination angle was smaller than that of the torso. Similar trends were observed in both THUMS and volunteer test data. Based on the comparison results, the study assumed that the occupant model represented by the THUMS Version 5 was capable of simulating the posture change due to steering with a lateral acceleration up to 1 g.

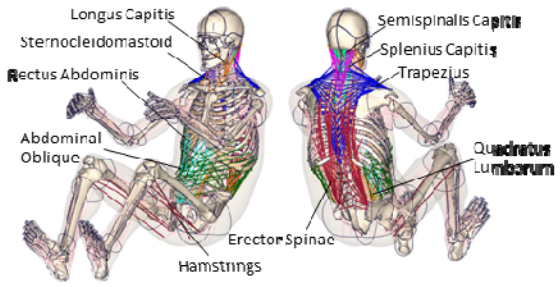

Fig. 1. THUMS Version 5 AM50 Occupant Model.

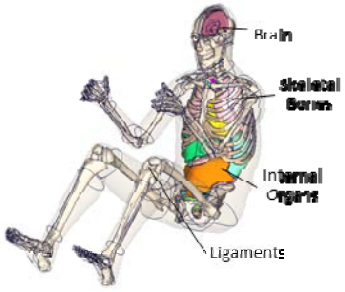

Fig. 2. THUMS Version 4 AM50 Occupant Model.

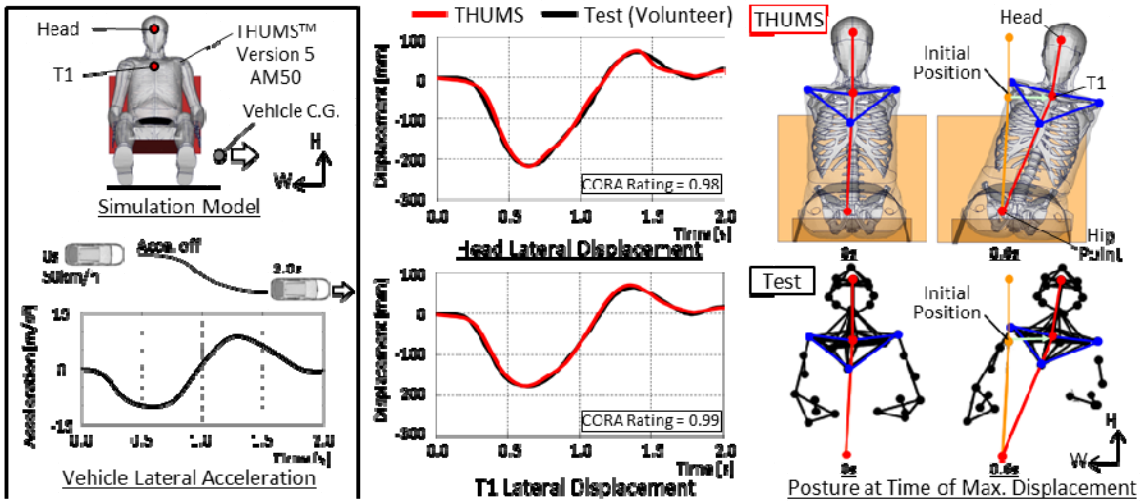

Fig. 3. Comparison of Response between THUMS and Volunteer during Lane Change.

The THUMS Version 4 precisely represents the human anatomy including the major skeletal parts, articular ligaments, brain, internal organs and other soft tissue parts. The model is capable of simulating impact kinematics and crash-induced injuries of occupants and pedestrians in vehicle collisions. The mechanical responses of the THUMS Version 4 against various impacts were validated to the test data with Post Mortem Human Subjects (PMHSs) described in the literature [14-17]. The model validations were performed from the head to the foot. The whole body kinematics in frontal and lateral collisions were also examined in comparison to the PMHS test data described in the literature [16-17].

Vehicle Model

Figure 4 shows the vehicle model representing the front part of the cabin. The study assumed that the cabin deformation was negligible in the front collisions. Rigid materials were assumed for the side sill, pillar, front header, door frame, windshield and floor. The deformation of the cabin in the side collision was simulated by applying prescribed displacements to the side sill, centre pillar and door frames. The interior parts that could come into contact with the occupant, such as the steering wheel, instrument panel, seat, seatbelt and airbag were assumed to be deformable. The seatbelt retractor model simulated the functions of a 2 kN Pre-tensioner and a 4 kN Load-limiter. In the case when the PSB was activated, a constant tensile force of 65 N was given to the seatbelt from the beginning of the pre-collision phase. The study assumed that the PSB could be activated when a forward obstacle was detected and/or when the driver made a sudden steering manoeuvre. The airbag

deployment was also simulated in the collision phase. The model included a driver airbag (DAB), a knee airbag (KAB), a side airbag (SAB) and a curtain airbag (CAB).

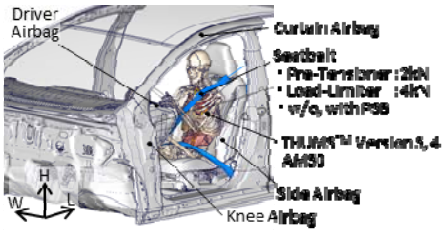

Fig. 4. Vehicle Cabin Model.
(Door was illustrated by wire-frame.)

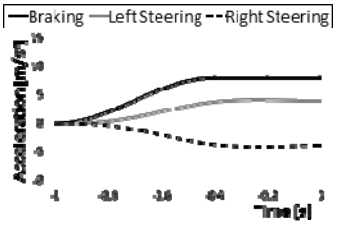

Fig. 5. Vehicle Acceleration in Pre-collision Phase.

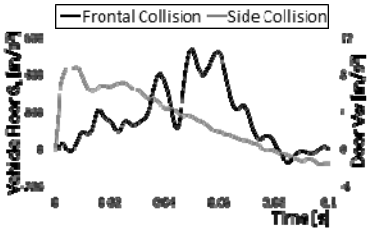

Fig. 6. Vehicle Acceleration and Door Velocity in Collisions.

Simulation Matrix

The pre-collision phase assumed three patterns of evasive manoeuvres: braking, left steering and right steering. The THUMS Version 5 was seated in the common driving position. Forward acceleration (deceleration) was applied to the cabin model to simulate the braking while lateral acceleration was applied for steering. Figure 5 shows the time history curves of the forward and lateral accelerations representing the evasive manoeuvres. The maximum deceleration generated by braking was assumed to be 0.8 g based on the survey on emergency braking in actual traffic accidents [4]. The maximum lateral acceleration caused by the steering was assumed to be 0.4 g based on the measurement in vehicle lane change tests [5]. The collision phase assumed a frontal collision and a side collision. A full overlap frontal collision at a speed of 56 km/h was assumed for the frontal collision simulation. A Pole side collision at a speed of 32 km/h (collision angle: 75 degrees) was assumed for the side collision simulation. Vehicle crash pulses were applied to the cabin model to simulate the frontal and side collisions. The THUMS Version 4 was placed on the driver's seat. In the cases with evasive manoeuvres, the occupant posture change obtained in the pre-collision phase with THUMS Version 5 was reproduced before initiating the vehicle crash pulse in the collision phase. The posture change generated a tensile force in the seatbelt and a compressive force in the seat cushion. The collision simulations were performed including such influence in the surrounding parts. For the cases with evasive manoeuvres, the collision simulations were conducted for both with and without activating the PSB. Figure 6 shows the vehicle crash pulse used for the frontal collision and the prescribed door deformation time history curve used for the side collision. TABLE I summarises all 14 cases.

TABLE I
SIMULATION MATRIX

Case No.	Pre-collision phase	Collision phase	
	Evasive Avoidance	Direction	PSB Activation
1	No Avoidance	Frontal Collision	No (without)
2	Braking		
3	Left Steering		
4	Right Steering		
5	Braking		Yes (with)
6	Left Steering		
7	Right Steering		
8	No Avoidance	Side Collision	No
9	Braking		
10	Left Steering		
11	Right Steering		
12	Braking		Yes
13	Left Steering		
14	Right Steering		

TABLE II
LIST OF IARV

IAV			IARV
HIC15		[-]	700
BrIC		[-]	1.05
Chest Deflection	Frontal	[mm]	49.6
	Lateral	[mm]	56.3
Abdomen Deflection		[mm]	88.6
Femur Force		[kN]	8.6
Sacroiliac Force		[kN]	5.1
Pubic Force		[kN]	3.2

The coordinate values of the nodes at the head, T1, T12 and hip point were measured to monitor the occupant motion. Those were calculated and converted into the vehicle reference coordinate system; longitudinal direction: L, width direction: W and height direction: H. The displacement in each direction was

calculated assuming that the initial point without evasive manoeuvres was the origin (zero). The injury assessment values (IAV) were calculated from nodes motion or section forces. The HIC and Brain Injury Criterion (BrIC) values were calculated using the acceleration and the angular velocity, respectively, at the head centre of gravity. The chest deflection in the frontal collision was recorded as the maximum value of three points at the upper, middle and lower portion of the sternum. The chest deflection in the side collision was represented by the maximum deflection of Rib 1-10. The abdominal deflection was defined as the maximum value of the abdominal epidermis. The femur force, sacroiliac force and pubic force were calculated as the maximum value of the force transmitting through the cross sections defined in the bones. The calculated IAV was normalised by dividing by the injury assessment reference value (IARV). The IARV was set to the value at which the injury risk was 50% as shown in TABLE II [18].

III. RESULTS

Pre-collision Phase

Figure 7 shows the occupant postures with and without evasive manoeuvres at the time of maximum head displacement. The upper body moved forward and came close to the steering wheel in the case of braking (for Cases 2 and 9). The maximum forward displacement of the head was 112 mm. The upper body moved toward the centre of the cabin in the left steering case (for Cases 3 and 10). The shoulder belt was located at the distal end of the clavicle due to the lateral motion. The maximum displacement of the head was 173 mm in the right direction. The upper body moved toward the door in the right steering case (for Cases 4 and 11). The shoulder belt came close to the neck. The maximum displacement of the head was 155 mm in the left direction. In the cases where the PSB was activated, the maximum displacement of the head was smaller than those without PSB activation. It was 79 mm forward in the braking case (for Cases 5 and 12), 93 mm rightward in the left steering case (for Cases 6 and 13) and 80 mm leftward in the right steering case (for Cases 7 and 14).

Figure 8 shows the time history curves of the seatbelt pull-out length and the shoulder belt path at the time of collision in the braking cases with and without activating the PSB. When the PSB was activated (for Cases 5 and 12), the seatbelt was retracted prior to the collision which resulted in a smaller pull-out length compared to the case without (for Cases 2 and 9). The length of the shoulder belt with the PSB was shorter than that without. The T1 forward displacement was smaller.

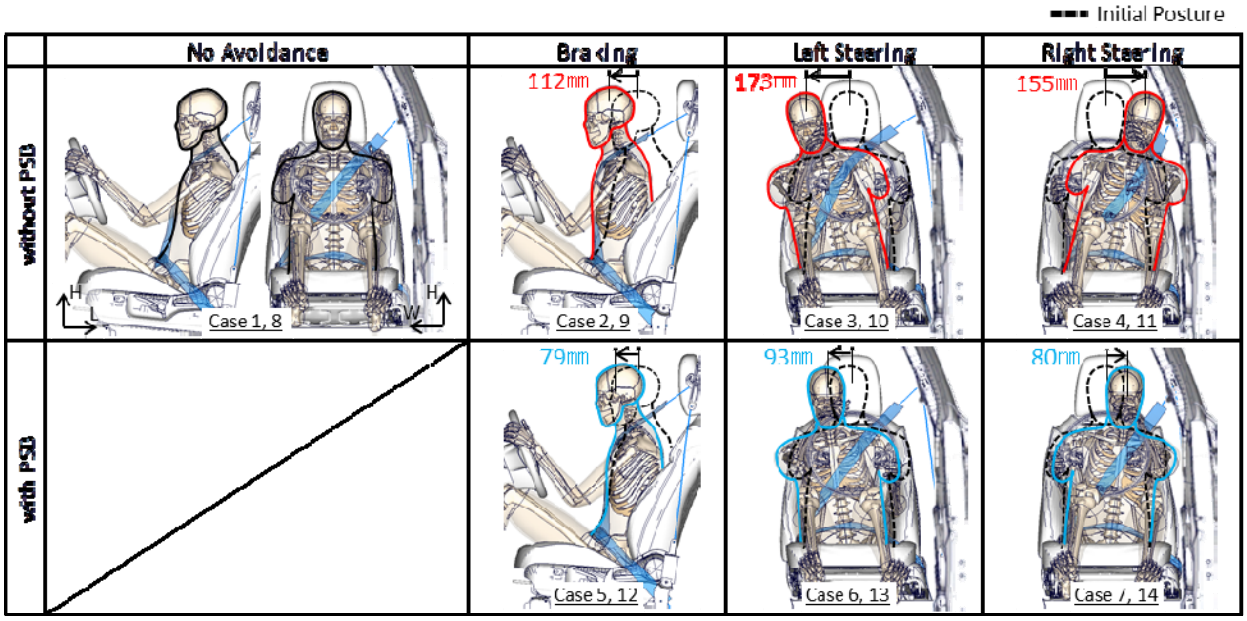

Fig. 7. Occupant Postures with and without Evasive Manoeuvres at Time of Maximum Head Displacement.

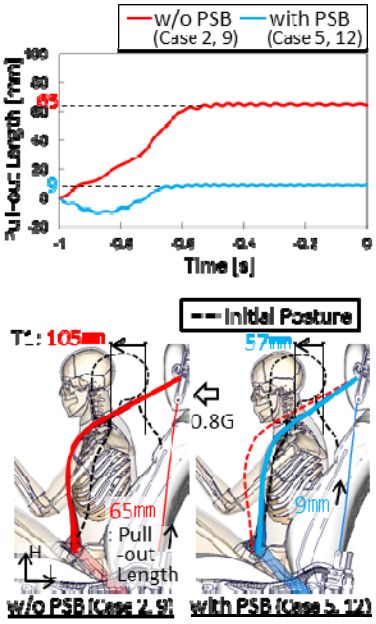

Fig. 8. Seatbelt Pull-out Length and Shoulder Belt Path in Braking Cases.

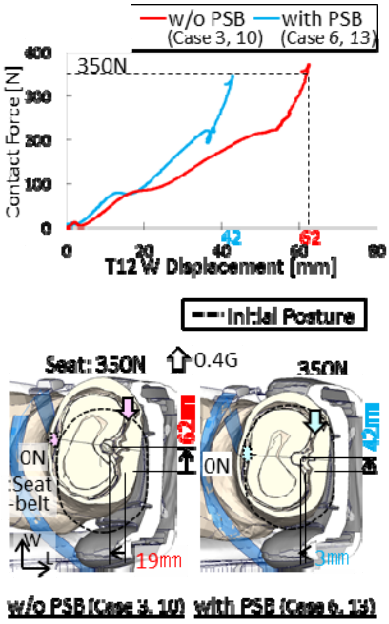

Fig.9. Force-Displacement Curves and Chest Motions (T12 Height Section) in Left Steering Cases.

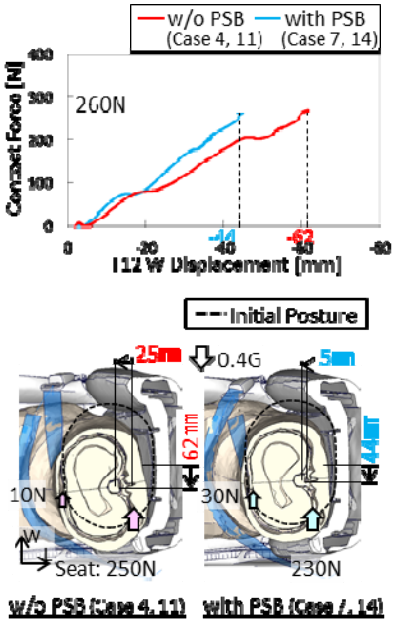

Fig.10. Force-Displacement Curves and Chest Motions (T12 Height Section) in Right Steering Cases.

Figure 9 shows the force-displacement curves and the chest motions in the horizontal section view with and without the PSB in the left steering cases. The vertical axis is the contact force acted from the seatbelt and the seat to the occupant torso while the horizontal axis is the T12 lateral displacement. In the case where the PSB was activated (for Cases 6 and 13), the slope of the curve was steeper and the maximum displacement was smaller compared to those without (for Cases 3 and 10). The chest moved forward as well as laterally. The seatbelt did not restrain the lateral motion. However, the forward displacement with the PSB was smaller than that without. The overlap ratio between the chest and the seatback side bolster was higher in the case with PSB. The force magnitudes and directions are also indicated in the figure. There was no substantial difference between the cases with and without the PSB. Figure 10 shows the force-displacement curves and the chest motions in the horizontal section view with and without the PSB for the right steering cases. In the case where the PSB was activated (for Cases 7 and 14), the slope of the curve was steeper and the maximum displacement was smaller compared to those in the case without (for Cases 4 and 11). Similarly, in the left steering cases, the chest moved both forward and laterally. The forward displacement with the PSB was smaller than that without. The overlap ratio between the chest and the seatback side bolster was higher in the case with PSB. The force magnitudes and directions are also indicated in the Fig. 10. The seatbelt restrained the lateral motion engaging the upper portion of the shoulder close to the neck. The magnitude of the contact force was 30 N in the case with the PSB while it was 10 N in the case without.

Frontal Collision

Figure 11 shows the occupant motion in the top and lateral views at the time of maximum head displacement for all the frontal collision cases. The numbers in the figure indicate the amount of head forward and lateral displacements from the initial position. In Case 1 where there was no evasive manoeuvres or activation of PSB, the occupant was positioned in the centre of the seat at the time of collision, then moved straight forward during the collision. The head contacted the centre of DAB and the chest was restrained by the shoulder belt. In Case 2, braking without PSB, the occupant head moved straight forward in the frontal collision. The head contact point was close to the centre of the airbag. In Case 3, left steering without PSB, the occupant was displaced to the right at the time of collision. The left shoulder slipped out of the seatbelt when the occupant moved forward in the frontal collision. The head contacted the edge of DAB and came close to the steering wheel. In Case 4, right steering without PSB, the head contacted the edge of DAB similarly to Case 3 but the shoulder did not slip out of the seatbelt. In Case 5, braking with PSB, the occupant moved straight forward similarly to Case 2. In Case 6, left steering with PSB, the head contacted the centre of DAB. The head motion was

smaller than that in Case 3 (left steering without PSB). In Case 7, right steering with PSB, the head contact point was close to the centre of DAB. The head motion was smaller than that in Case 4 (right steering without PSB).

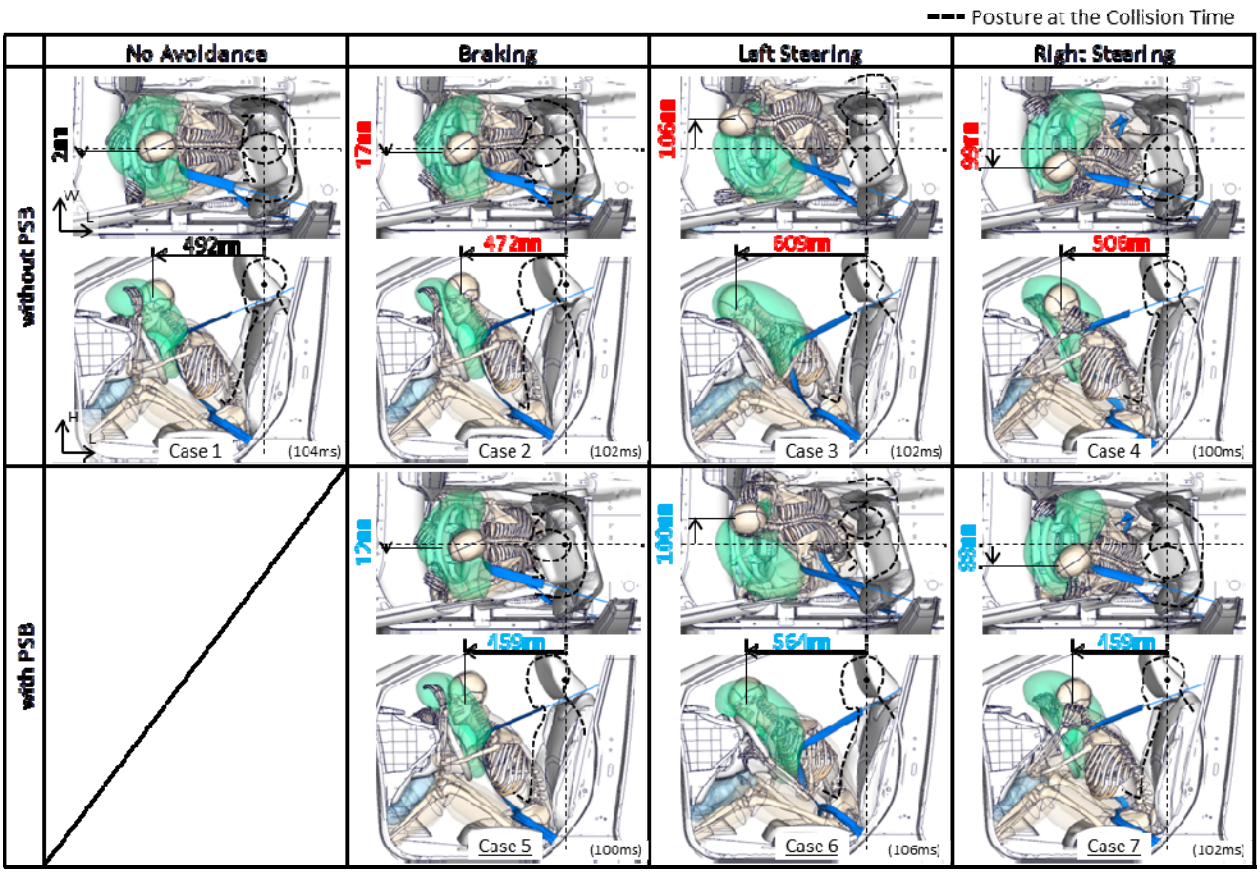

Fig. 11. Occupant Motions at Time of Maximum Head Displacement in Frontal Collision.

Figure 12 shows the IAV/IARV ratios. When the PSB was not activated, the HIC ratio in Case 3 (left steering) was higher than that in Case 1 (without evasive manoeuvres) while those in Case 2 (braking) and Case 4 (right steering) were lower. When the PSB was activated, the HIC ratios in Case 5 (braking) and Case 6 (left steering) were lower than those without the PSB while that in Case 7 (right steering) was higher. When the PSB was not activated, the BrIC ratios in Cases 2-4 (with evasive manoeuvres) were higher than that in Case 1 (without evasive manoeuvres). The ratio was the highest (0.99) in Case 4 (right steering). When the PSB was activated, the BrIC ratios in Case 5 (braking) and Case 7 (right steering) were lower than those without activating the PSB while that in Case 6 (left steering) was higher. When the PSB was not activated, the ratios of chest deflection in Case 2 (braking) and Case 3 (left steering) were higher than that in Case 1 (without evasive manoeuvres) while that in Case 4 (right steering) was lower. When the PSB was activated, the ratios of chest deflection in Cases 5-7 (with evasive manoeuvres) were higher than those in Cases 2-4 (with evasive manoeuvres). When the PSB was not activated, the ratios of abdomen deflection in Cases 2-4 were higher than that in Case 1. When the PSB was activated, the ratios of abdomen deflection in Case 5 (braking) and Case 6 (left steering) were higher than those without activating the PSB while that in Case 7 (right steering) was lower. When the PSB was not activated, the ratios of femur force in Case 2 (braking) and Case 3 (left steering) were lower than that in Case 1 (without evasive manoeuvres) while that in Case 4 (right steering) was higher. When the PSB was activated, the ratios of femur force in Cases 5 (braking) and Case 7 (right steering) were lower than those without activating the PSB while that in Case 6 (left steering) was higher. Note that all the IRV values were below the IARV values in the fontal collision cases simulated in this study. Figure 13 shows the time history curves of the head acceleration in Cases 1, 3 and 6. Note that the HIC ratio in Case 3 (left steering without PSB) was higher than that in Case 1 (without evasive manoeuvres) while that in Case 6 (left steering with PSB) was lowered by activating the PSB. The magnitude of acceleration during the first rise (0.04 to 0.07 second) in Case 3 was lower than that in Case 1. The peak was higher in Case 3. The initial rise in Case 6 was higher than that in Case 3. The peak was lower in

Case 6. In Case 1, the head contacted the centre of DAB and stopped before reaching the steering wheel. In Cases 3 and 6 the head came close to the steering wheel. However, the head motion in Case 6 (with PSB) was smaller than that in Case 3 (without PSB). Figure 14 shows the time history curves of the head angular velocities around three axes (X, Y, Z) in Cases 1, 4 and 7. Those were calculated in the head local coordinate system. Note that the BrIC ratio in Case 4 (right steering) was the highest. The angular velocities around X and Z axes in the latter stage of collision (0.12 to 0.13 second) in Case 4 were higher than those in Case 1. The curves in Case 7 (with PSB) were close to those in Case 4 (without PSB).

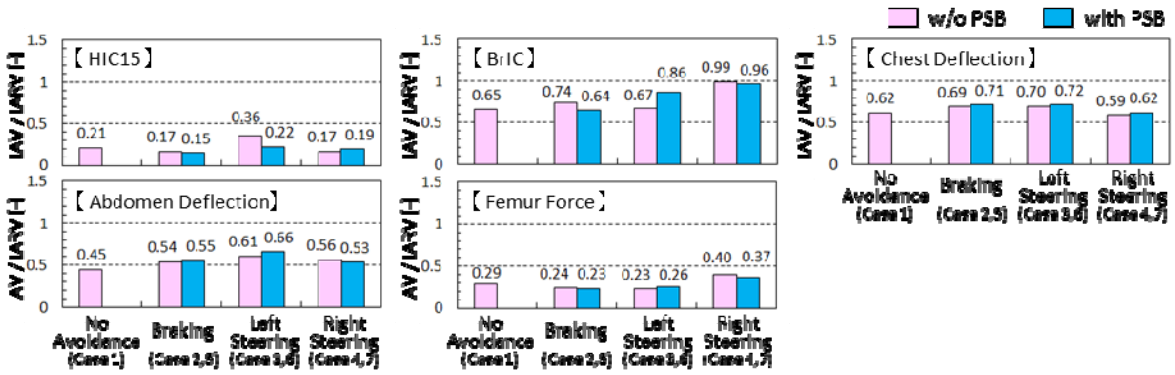

Fig. 12. IAV/IARV Ratios in Frontal Collision.

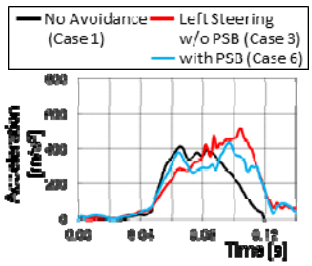

Fig. 13. Head Acceleration in Cases 1, 3 and 6.

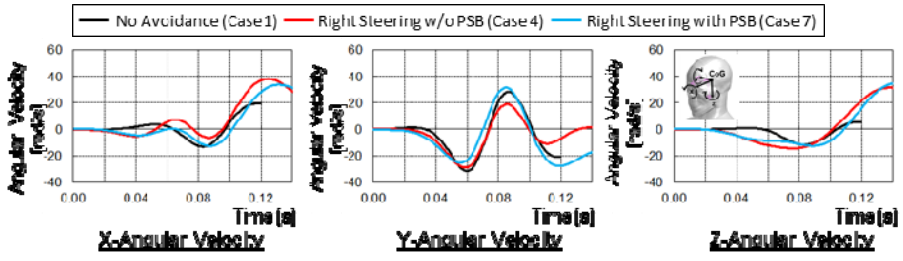

Fig. 14. Head Angular Velocity in Cases 1, 4 and 7.

Side Collision

Figure 15 shows the occupant motion in the front and lateral views at the time of maximum lateral displacement of the head for all the side collision cases. The figure compares the cases between with and without evasive manoeuvres and with and without PSB. The displacement values indicate the head forward and lateral displacements measured from the initial position. In Case 8, without evasive manoeuvre or PSB, the CAB deployed and restrained the head while the SAB developed and restrained the chest. In Case 9, braking without PSB, the upper body moved forward before the collision and the chest contacted the front edge of SAB in the side collision. In Case 10, left steering without PSB, the upper body moved toward the centre of the cabin. The head and chest travelled longer distances during the side collision than in Case 8. The head was restrained by CAB while the chest was restrained by SAB. In Case 11, right steering without PSB, the upper body came close to the door before the collision. There was a relatively small space for CAB deployment. The head came close to the pole. A similar situation was observed for SAB. The deployed geometry was shifted to the posterior side of the occupant. However, the torso side was covered by the front portion of SAB. In Case 12, braking with PSB, the forward motion of the occupant was smaller than that in Case 9 without the PSB. The overlap between the chest and SAB in Case 12 was larger than that in Case 9. Similar head kinematics was observed in the two cases. In Case 13, left steering with PSB, the upper body of the occupant was already close to the door at the beginning of collision. The head moved toward the door and was restrained by CAB while the chest was restrained by SAB. In Case 14, right steering with PSB, the lateral distance of the occupant from the door was greater than that in Case 11 without PSB at the time of collision. The CAB developed between the head and the door and restrained the head.

Figure 16 shows the IAV/IARV ratios. In the cases with evasive manoeuvres (Cases 9-11), both HIC ratios and BrIC ratios were higher than those without (Case 8). The HIC ratio in Case 11 (right steering) and the BrIC ratio in Case 10 (left steering) were higher than 1.0. When the PSB was activated, the ratios were lower than those without PSB except Case 13. Relatively high chest deflection ratios were noted in Case 9 (braking) and Case 11 (right steering) but were below 1.0. When the PSB was activated, the chest deflection ratio in Case 12 (braking) was lower than that without (Case 9) while those in Case 13 (left steering) and Case 14 (right steering) were higher than those without (Cases 10 and 11). The pubic force ratio in Case 11 (right steering) was higher than that in Case 8 (without evasive manoeuvres) while those in the other cases were lower. When the PSB was activated, the pubic ratio in Case 14 (right steering) was lower than that without (Case 11) while those in Case 12 (braking) and Case 13 (left steering) were higher than without (Cases 9 and 10). The iliac force ratios with the evasive manoeuvres (Cases 9-11) were higher than that without (Case 8). When the PSB was activated, the iliac force ratios were lower than those without in all the cases. Note that all the IRV values with the PSB were below the IARV values in the side collision cases simulated in this study.

Figure 17 shows the time history curves of the head angular velocity around three axes (X, Y, Z) in Cases 8, 10 and 13. Note that the BrIC value in Case 10 (left steering) was the highest. The angular velocities around X and Z axes in Case 10 were higher than those in Case 8 (without evasive manoeuvres). The negative peaks of angular velocities around X and Z axes in Case 13 where the PSB was activated were smaller than those in Case 10 (without PSB).

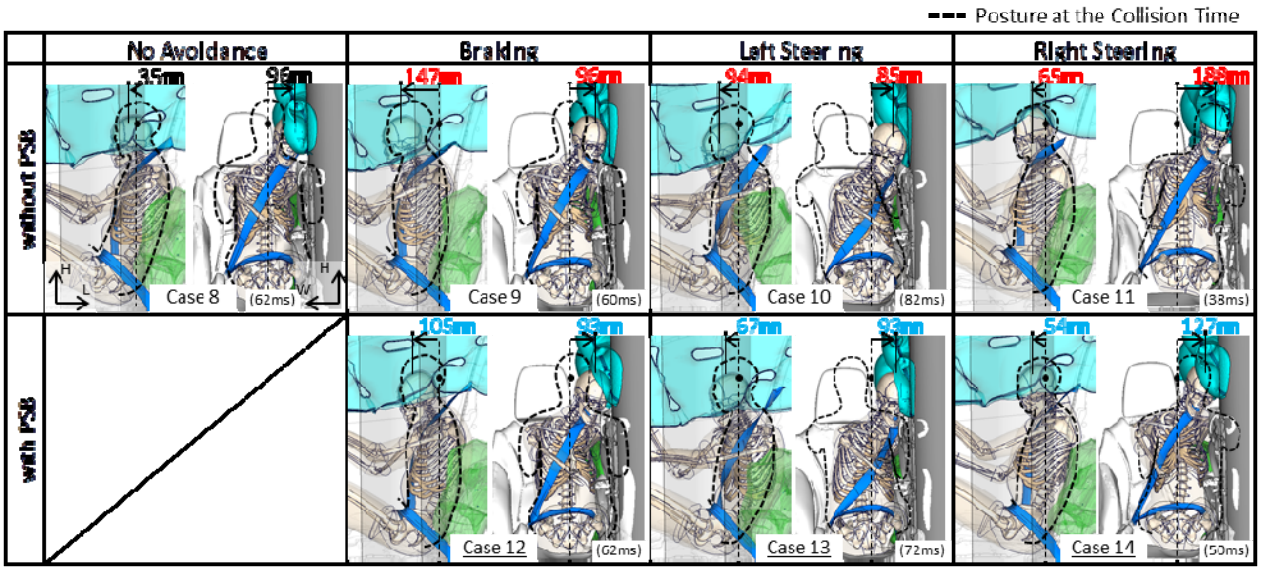

Fig. 15. Occupant Motions at Time of Maximum Head Displacement in Side Collision.

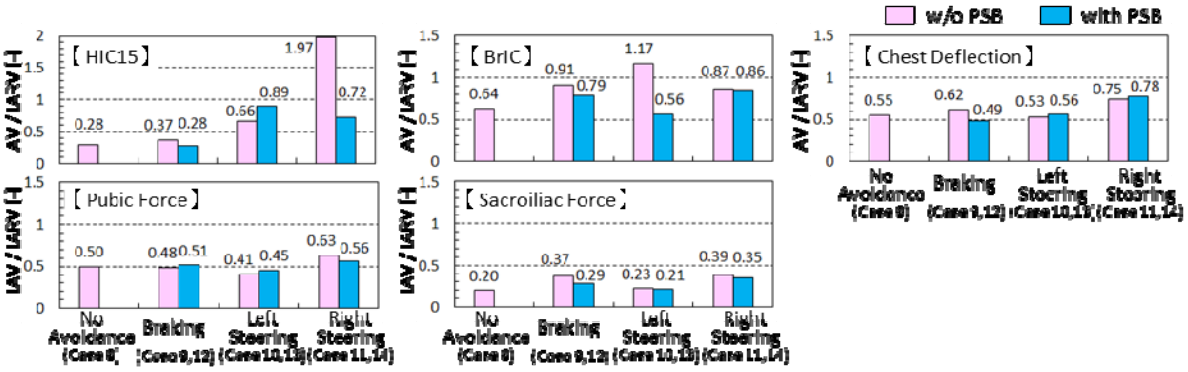

Fig. 16. IAV/IARV Ratios in Side Collision.

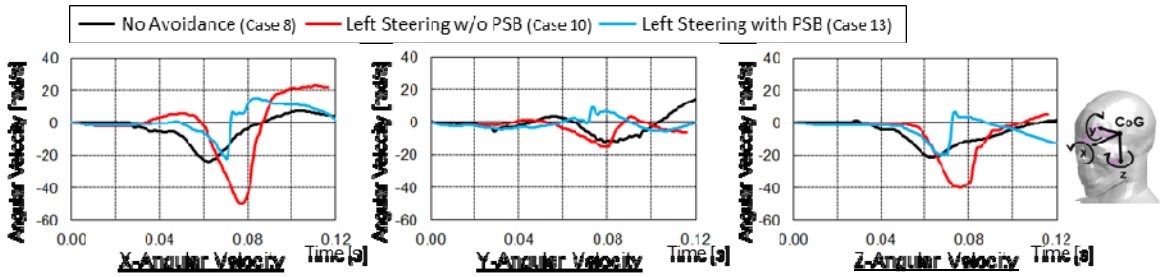

Fig. 17. Head Angular Velocity in Cases 8, 10 and 13.

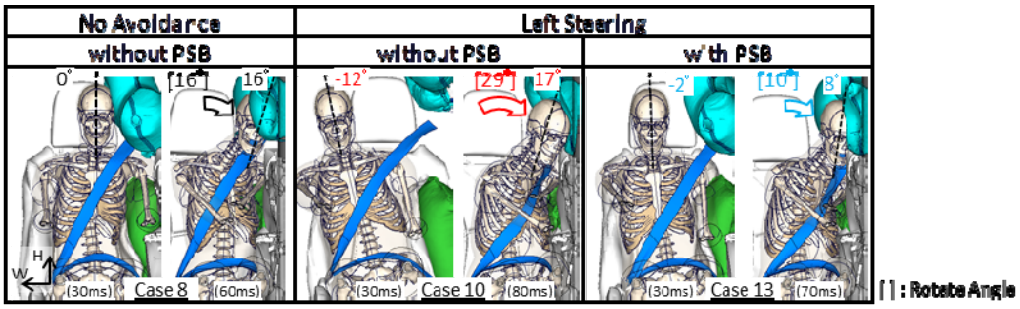

Fig. 18. Occupant Head Motions at 0.03 [s] and at Time of Maximum Angular Velocity in Cases 8, 10 and 13.

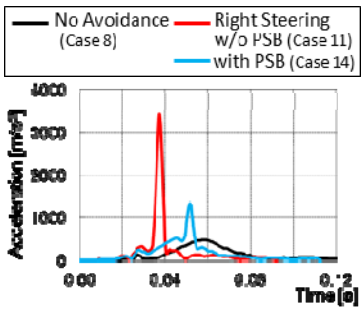

Fig. 19. Head Acceleration in Cases 8, 11 and 14.

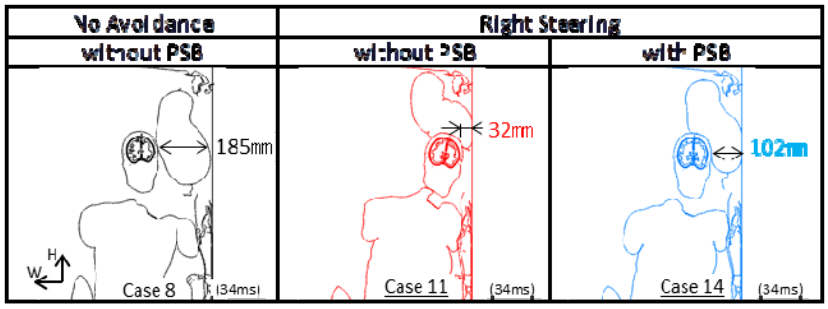

Fig. 20. Occupant Motions in Coronal Section at Time of Deployment CAB in Cases 8, 11 and 14.

Figure 18 shows the occupant head motions in the frontal view before generating the head angular velocity (0.03 second) and at the time of maximum angular velocity in Cases 8, 10 and 13. The angle values in the figure shows the angles relative with respect to vehicle H (vertical) axis and the angle change between the two time frames in each case. In Case 10 (left steering), both head angle and angle change at 0.03 second were greater than those in Case 8. In Case 13 when the PSB was activated, both head angle and angle change at 0.03 second and at the timing of maximum angular velocity were smaller than those without the PSB (Case 10). Figure 19 shows the time history of the head acceleration in Cases 8, 11 and 14. Note that the HIC ratio in Case 11 (right steering) was the highest among all the cases. The magnitude of head acceleration right after the airbag deployment (0.02 to 0.03 second) in Case 11 was higher than that in Case 8 (without evasive manoeuvres). In Case 11, the timing of the peak acceleration was earlier and the maximum acceleration was higher than those in Case 8. In Case 14 where the PSB was activated, the timing of peak acceleration was later and the maximum acceleration was lower than those without (Case 11). Figure 20 compares the occupant motions in the front view among Cases 8, 11 and 14. The geometry is displayed in the coronal cross section passing through the head centre of gravity at the timing of airbag maximum deployment (0.034 second). In Case 8, the CAB developed between the head and the pole with a width of 185 mm for deployment. In Case 11 (right steering) the head position was close to the door at the beginning of collision. The width for CAB deployment was 32 mm, which was smaller than that in Case 8. In Case 14 where the PSB was activated, the width for CAB deployment was 102 mm which was greater than that in Case 11.

IV. DISCUSSION

In the case of braking, the seatbelt webbing was pulled out from the retractor as the occupant moved forward. The emergency locking retractor (ELR) was activated to lock the shaft in the retractor. The occupant body stopped when the seatbelt load balanced with the inertial load. The ELR was not activated in the case of steering. There was some distance between the chest and the seatback side bolster in the initial position. The chest moved laterally due to steering and reached the side bolster of the seatback. The torso compressed the foam material of the bolster generating load. The occupant body stopped when the compressive load balanced with the inertial load. As a result, the lateral displacement of the occupant due to the steering was greater than the forward displacement due to the braking despite its lower acceleration level. In the case of right steering, the shoulder belt supported the upper part of the shoulder. That helped lower the magnitude of the compressive load balancing with the inertial load of the occupant.

In the frontal collision cases, the calculated IRV values were below the IARV values. A relatively high HIC ratio (0.36) was noted in Case 3 (left steering without PSB). The occupant shoulder slipped out of the seatbelt due to the lateral motion before collision as observed in Fig. 11. The head contacted the edge of the DAB and came close to the steering wheel. Such a head motion raised the HIC ratio in Case 3. On the other hand, the occupant shoulder was kept engaged with the seatbelt in Case 4 (right steering without PSB). The head forward displacement was smaller than that in Case 3. As a result, the HIC ratio was relatively low. However, the BrIC ratio was the highest in Case 4. It is considered that the head was more rotated due to the shoulder engagement. In the side collision cases, the influence of occupant posture change on injury values was relatively high. In Case 11 where the HIC ratio was the highest, the occupant upper body came close to the door due to the right steering. There was relatively less space for CAB deployment compared to that in Case 8 (without evasive manoeuvres) as shown in Fig. 15. The high acceleration peak was generated because the CAB covered only the superior portion of the head as shown in Fig. 19 and 20. In Case 10, where the BrIC ratio was the highest, the occupant upper body moved away from the door due to the left steering. During the side collision, the head moved toward the door and rotated largely after the shoulder contacted the door as shown in Fig. 18. The large rotation resulted in a high BrIC ratio. The influence of occupant posture change on the injury values in the side collisions was greater than that in the frontal collisions. The initial distance between the occupant head and the cabin interior parts was approximately 500 mm in the forward direction and approximately 250 mm in the lateral direction. The head forward displacement due to braking was approximately 100 mm while the lateral displacement due to the steering was approximately 150 mm for both left and right directions. The ratio of the head displacement to the initial distance was grater in the lateral direction than that in the forward direction. It is considered that the greater ratio resulted in the high sensitivity of occupant posture change in the side collisions.

When the PSB was activated, the lateral as well as the forward motion, of the occupant was reduced. In Case 3 (left steering without PSB), the chest moved forward along the seatback side bolster as shown in Fig. 9. Because the PSB restrained the forward motion, the chest was pushed against the side bolster and resulted in the small lateral distance. The IAV/IARV ratios were lower than 1.0 in all the cases with the PSB. There was a great reduction of the HIC ratio from Case 11 to Case 14 (right steering). The reduction of the BrIC ratio was the largest from Case 10 to Case 13 (left steering). The reduction of occupant posture change by the PSB helped lower the IAV/IARV ratios.

V. LIMITATIONS

The results obtained in this study were based on specific evasive manoeuvres, collision conditions and occupant size while those in actual collisions vary. This study assumed a response surface for muscle activation which represented the mean data of the test subjects reported in the literature. Actual muscle response could change depending on the situation even in the same occupant. Thus, further studies are necessary to take into account such variations of occupant reposes especially in the pre-collision phase. Moreover, the posture change of the occupant model was only verified for the cases without the PSB. It was considered that the model was capable of simulating the posture change with the PSB against the small pre-crash seatbelt force assumed in this study.

VI. CONCLUSIONS

The occupant posture changes due to the evasive manoeuvres were simulated using THUMS. The influence of posture change on the impact kinematics and the injury values during collisions were investigated. The effect of PSB on injury values was also examined. The occupant head moved forward when braking while it moved laterally when steering. In the frontal collision after steering, the head did not contact the centre of DAB. The maximum forward displacement became greater than that without steering. In the side collision after steering, the head position at the time of collision affected the impact kinematics. The occupant changing posture also affected HIC and BrIC. The HIC value became high when the occupant head came close to the interior parts. The BrIC value became high when the occupant head rotated largely and rapidly. The PSB reduced the forward motion of the occupant prior to the collision. The lateral motion was also reduced as the chest moved forward along the seatback surface. When the PSB was activated, the increased HIC and BrIC values were lower than those without PSB activation by the reduction of the occupant posture change.

VII. REFERENCES

[1] Accident Analysis Report, *Institute for Traffic Accident Research and Data Analysis*, Tokyo, Japan, 2005.

[2] Yamamoto A. Active safety based on average driver's behavior, *International Association of Traffic and Safety Science Review*, 1998, 24(2): 70-78.

[3] Doi S, Nagiri S, Amano Y. Analysis of active safety performances of automobile based on driving maneuvers in emergent situations. *TOYOTA CENTRAL R&D LABS., INC. Review*, 1998, 33(1): 31-38.

[4] Schoeneburg R, Baumann K, Fehring M. The efficiency of PRE-SAFE systems in pre-braked frontal collision situations. *Proceedings of the 22nd ESV Conference*, 2011, Washington, D.C., USA.

[5] Araszewski M, Toor A, Overgaard R, Johal R. Lane change maneuver modeling for accident reconstruction applications. *Society of Automobile Engineers*, 2002, Paper No. 2002-01-0817.

[6] Ólafsdóttir J M, Östh J K H et al. Passenger kinematics and muscle responses in autonomous braking events with standard and reversible pre-tensioned restraints. *Proceedings of IRCOBI Conference*, 2013, Gothenburg, Sweden.

[7] Huber P, Christova M et al. Muscle activation onset latencies and amplitudes during lane change in a full vehicle test. *Proceedings of IRCOBI Conference*, 2013, Gothenburg, Sweden.

[8] Huber P, Kirschbichler S, Prüggler A, Steidl T. Passenger kinematics in braking, lane change and oblique driving maneuvers. *Proceedings of IRCOBI Conference* , 2015, Lyon, France.

[9] Meijer R, Elrofai H, Broos J, Hassel E V. Evaluation of an active multi-body human model for braking and frontal crash events. *Proceedings of the 23rd ESV Conference*, 2013, Seoul, Republic of Korea.

[10] Yamada K, Gotoh M et al. Simulation of occupant posture change during autonomous emergency braking and occupant kinematics in frontal collision. *Proceedings of IRCOBI Conference*, 2016, Malaga, Spain.

[11] Ito D, Ejima S et al. Occupant kinematic behavior and effects of a motorized seatbelt on occupant restraint of human volunteers during low speed frontal impact. *Proceedings of IRCOBI Conference*, 2013, Gothenburg, Sweden.

[12] Gehre C, Gades H, Wernicke P. Objective rating of signals using test and simulation response. *Proceedings of the 21st ESV Conference*, 2009, Stuttgart, German.

[13] International Organization for Standardization, Road vehicles - Objective rating metric for non-ambiguous signals, ISO/TS 18571, Geneva, Switzerland, 2014.

[14] Watanabe R, Miyazaki H, Kitagawa Y, Yasuki T. Research of the relationship of pedestrian Injury to collision speed, car-type, impact location and pedestrian sizes using human FE model (THUMS Version 4). *Stapp Car Crash Journal*, 2012, 561: 269-32.

[15] Shigeta K, Kitagawa Y, Yasuki T. Development of next generation human FE model capable of organ injury prediction. Proceedings of the 21st ESV Conference, 2009, Stuttgart, German.

[16] Kitagawa Y, Yasuki T. Correlation among seatbelt load, chest deflection, rib fracture and internal organ strain in frontal collisions with human body finite element models. *Proceedings of IRCOBI Conference*, 2013, Gothenburg, Sweden.

[17] Kitagawa Y, Hayashi S, Yamada K, Gotoh M. Occupant kinematics in simulated autonomous driving vehicle collisions, direction and angle. *Stapp Car Crash Journal*, 2017, 61: 101-155.

[18] NHTSA's new car assessment program - Request for comments. Federal Register: 78522-78591, *NHTSA*, Washington, D.C., USA, 2015.